

Photochemistry of 1-(*N,N*-Diethylamino)diazen-1-ium-1,2-diolate: An Experimental and Computational Investigation

Christopher M. Pavlos,[†] Andrew D. Cohen,[†] Raechelle A. D'Sa,[†] R. B. Sunoj,[‡]
Walter A. Wasylenko,[†] Preeya Kapur,[†] Heather A. Relyea,[†] Neema A. Kumar,[†]
Christopher M. Hadad,^{*,‡} and John P. Toscano^{*,†}

Contribution from the Department of Chemistry, Johns Hopkins University,
3400 North Charles Street, Baltimore, Maryland 21218, and Department of Chemistry,
The Ohio State University, 100 West 18th Avenue, Columbus, Ohio 43210

Received February 4, 2003; E-mail: jtoscانو@jhu.edu; hadad.1@osu.edu

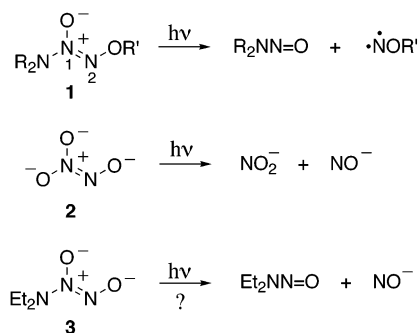
Abstract: The aqueous photochemistry of the sodium salt of 1-(*N,N*-diethylamino)-diazen-1-ium-1,2-diolate (**3**) has been investigated by both experimental and computational methods. Photolysis results in the formation of the *N*-nitrosodiethylamine radical anion (**5**) and nitric oxide (NO) via a triplet excited state. The nitrosamine radical anion either undergoes electron transfer with NO before cage escape to form triplet NO⁻ and nitrosamine (minor process) or rapidly dissociates to form an additional molecule of NO and ultimately amine (major process). The production of nitrosamine radical anion **5** upon photolysis of diazeniumdiolate **3** is confirmed by low-temperature EPR spectroscopy. The calculated energetics for the ground and excited states of the parent diazeniumdiolate ion at the CIS and B3LYP levels of theory as well as B3LYP calculations on the fragmentation processes were very effective in rationalizing the observed photodissociation processes.

Introduction

Anions with the X[N(O)NO]⁻ (X = O⁻, CR₃, SO₃⁻, and NR₂) functional group have been used increasingly as probes for studying the biology of nitric oxide (NO) and nitroxyl (NO⁻/HNO) over the past decade, and have an expansive chemical history spanning two centuries.¹ 1-(*N,N*-Dialkylamino)diazen-1-ium-1,2-diolates (X = NR₂) are stable as solid salts, but release up to 2 mol of NO (plus 1 mol of amine) when dissolved in aqueous solution under physiologically relevant conditions.¹ To extend the usefulness and applications of these diazeniumdiolates as NO donors, we have developed efficient photosensitive protecting groups for these anions.² During the course of this work, we have demonstrated that the photochemistry of simple *O*²-alkyl- and *O*²-benzyl-substituted diazeniumdiolates **1** is complicated by a reaction that produces a potentially carcinogenic *N*-nitrosamine and a reactive oxynitrene intermediate (Scheme 1).³

The photochemistry of the sodium salt of ⁻O[N(O)NO]⁻, commonly known as Angeli's salt (**2**), has been previously

Scheme 1



studied.^{4,5} Photodecomposition of **2** results in generation of NO₂⁻ and NO⁻ (Scheme 1), a reaction with bond-breaking that is analogous to the nitrosamine/oxynitrene forming reaction observed for *O*²-substituted diazeniumdiolates.³ If such a reaction was important in the photochemistry of 1-(*N,N*-dialkylamino)diazeniumdiolates, the expected products would be nitrosamine and NO⁻ (Scheme 1), raising potential phototoxicity issues. We have investigated the photochemistry of the sodium salt of 1-(*N,N*-diethylamino)-diazen-1-ium-1,2-diolate (**3**) by both experimental and computational methods and report herein our results.

[†] Johns Hopkins University.

[‡] The Ohio State University.

- (1) For a recent review of the chemistry of diazeniumdiolate derivatives, see: Hrabie, J. A.; Keefer, L. K. *Chem. Rev.* **2002**, *102*, 1135–1154.
 (2) (a) Ruane, P. H.; Bushan, K. M.; Pavlos, C. M.; D'Sa, R. A.; Toscano, J. P. *J. Am. Chem. Soc.* **2002**, *124*, 9806–9811. (b) Bushan, K. M.; Xu, H.; Ruane, P. H.; D'Sa, R. A.; Pavlos, C. M.; Smith, J. A.; Celius, T. C.; Toscano, J. P. *J. Am. Chem. Soc.* **2002**, *124*, 12640–12641.
 (3) Srinivasan, A.; Kebede, N.; Saavedra, J. E.; Nikolaitchik, A. V.; Brady, D. A.; Yourd, E.; Davies, K. M.; Keefer, L. K.; Toscano, J. P. *J. Am. Chem. Soc.* **2001**, *123*, 5465–5472.

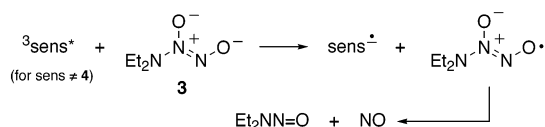
(4) Donald, C. E.; Hughes, M. N.; Thompson, J. M.; Bonner, F. T. *Inorg. Chem.* **1986**, *25*, 2676–2677.

(5) (a) Shafirovich, V.; Lyman, S. V. *Proc. Natl. Acad. Sci. U.S.A.* **2002**, *99*, 7340–7345. (b) Shafirovich, V.; Lyman, S. V. *J. Am. Chem. Soc.* **2003**, *125*, 6547–6552.

Table 1. Percent Yields of Products Following Rayonet Photolysis of **3** in Water^a

photolysis λ (nm)	purge	amine (NMR) ^b	NO ^c	nitrosamine (NMR) ^b	nitrosamine (HPLC) ^d	N ₂ O ^e
254	Ar	71	105	29	18	18
254	O ₂	71	<i>g</i>	29	21	<i>g</i>
300	Ar	90	158	10	10	<i>g</i>
300	O ₂	90	<i>g</i>	10	11	<i>g</i>
300	NO	90	<i>g</i>	10	<i>g</i>	<i>g</i>

^a Average of at least three measurements; based on percent reactant converted; estimated error $\pm 5\%$. ^b Amine and nitrosamine were analyzed by NMR spectroscopy following 30% conversion of 6.5 mM **3** in D₂O (pD ≥ 12). ^c NO was analyzed electrochemically following photolysis of **3** in H₂O (pH = 12). See Experimental Section for details. ^d Nitrosamine was analyzed by HPLC following 30% conversion of 0.1 mM **3** in H₂O (pH = 12). (Representative HPLC experiments performed in D₂O (pD ≥ 12) provided similar results.) ^e N₂O was analyzed by gas chromatography following 254 nm photolysis (100% conversion) of 1 mM **3** in H₂O (pH = 12). ^f 17% ONOO⁻ is observed by UV-vis spectroscopy ($\epsilon_{302} = 1670 \text{ M}^{-1} \text{ cm}^{-1}$)¹¹ following photolysis (100% conversion) of 0.2 mM **3** in H₂O (pH = 14). ^g Not determined.

Scheme 2**Results and Discussion**

Product Analysis. Products formed following aqueous photolysis of **3** were quantified by a variety of analytical methods (Table 1). NMR analysis of reaction mixtures showed diethylamine and *N*-nitrosodiethylamine as the only organic products formed. Yields of nitrosamine were also determined independently by HPLC analysis. NO was analyzed electrochemically; NO⁻/HNO was quantified indirectly by nitrous oxide (N₂O) or peroxyxynitrite (ONOO⁻) by gas chromatography or UV-vis absorption spectroscopy, respectively, as detailed below. As indicated in Table 1, nitrosamine is observed, but in much lower yields than initially anticipated.

Triplet Sensitization and Quenching Experiments. We also examined the effects of triplet sensitized photolysis on observed product distributions. Triplet sensitized photolysis of **3** with 4,4'-dihydroxybenzophenone (**4**) in D₂O (pD ≥ 12) has no effect on the yields of amine (90%) and nitrosamine (10%) relative to those observed following direct photolysis at 300 nm, suggesting that essentially all of the observed photochemistry occurs through ³**3***.

Triplet sensitized photolysis with other sensitizers of similar triplet energy, however, is complicated by a presumed electron transfer to the triplet excited sensitizer from **3** leading to Et₂NN(O)NO[•], which subsequently dissociates to nitrosamine and NO (Scheme 2). (B3LYP/6-31+G(d,p) calculations suggest that this dissociation is favored thermodynamically by 13.3 kcal/mol.) For example, sensitization with xanthone leads to 20% amine and 80% nitrosamine, but HPLC analysis shows significant decomposition of the xanthone. Sensitization with **4**, on the other hand, leads to no decomposition of the sensitizer. At pH = 12, one of the hydroxyl groups of **4** is deprotonated, presumably making the complicating electron-transfer process of Scheme 2 (to form a radical dianion) unfavorable.

As shown in Table 1, we examined the effect of oxygen as a triplet quencher. (Experiments with organic triplet quenchers

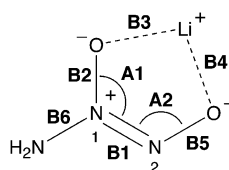
such as biacetyl and potassium sorbate were complicated by chemical reactivity.) Oxygen (1.3 mM in water⁶) has no effect on the relative yields of amine and nitrosamine, but we do observe decreased quantum yields for photodecomposition in oxygen- versus argon-saturated solutions following 266 and 300 nm photolysis: $\Phi(\text{Ar}) = 0.18$, $\Phi(\text{O}_2) = 0.068$ and $\Phi(\text{Ar}) = 0.02$, $\Phi(\text{O}_2) = 0.009$, respectively. These results are consistent with incomplete quenching of ³**3*** by oxygen (and presumably no photoreactivity via ¹**3***) under the conditions of our experiments.

Computational Studies. To gain further mechanistic insight into how the products reported in Table 1 are formed, we examined the structures of diazeniumdiolate S₀, S₁, and T₁ states via computational methods. Vertical excitation energies have been computed using time-dependent density functional theory (TD-DFT) and configuration interaction with all single excitations (CIS) methods⁷ on X[N(O)NO]⁻ (X = NH₂ and NMe₂) and the lithium complexes as model systems. Excitation energies were evaluated at the TD-DFT/B3LYP/6-31+G(d,p)//B3LYP/6-31+G(d,p) and CIS/6-31+G(d,p)//HF/6-31+G(d,p) levels. The qualitative trends for the vertical excited states were similar using both methods. Optimized geometries, orbital contour plots, computed vertical excitation energies (eV and nm), and oscillator strengths are provided as Supporting Information, as is the experimental absorption spectrum of **3**.

While both the lowest singlet excited state for H₂N[N(O)NO]⁻ as well as the corresponding lithium complex are $n \rightarrow \pi^*$ in character, the lowest triplet states are of $\pi \rightarrow \pi^*$ character. The π and π^* MOs involved in these transitions are primarily localized on the N₁-N₂ bond. More significant geometrical changes in this bond are thus expected for the ³($\pi \rightarrow \pi^*$) state as compared to the S₀ and S₁ singlet states. This is indeed observed for the optimized geometries of the excited states at the CIS/6-31+G(d,p) level (Table 2). The N₁-N₂ bond length for the ³($\pi \rightarrow \pi^*$) state is calculated to be 1.57 Å for T₁, as compared to 1.22 and 1.39 Å for the S₀ and ¹($n \rightarrow \pi^*$) states, respectively. Also, geometry optimizations of the ³($\pi \rightarrow \pi^*$) state for H₂N[N(O)NO]⁻ at the B3LYP/6-31+G(d,p) level resulted in a loose complex with an elongated N₁-N₂ bond length of 2.46 Å, suggesting a barrierless dissociation pathway for the lowest triplet excited state, presumably to nitrosamine radical anion and NO radical. Indeed, the calculated spin density distribution (Figure 1) is consistent with the formation of NO radical from the triplet dissociation pathway.

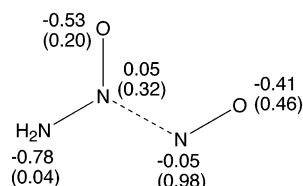
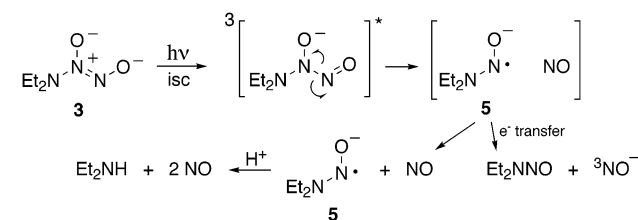
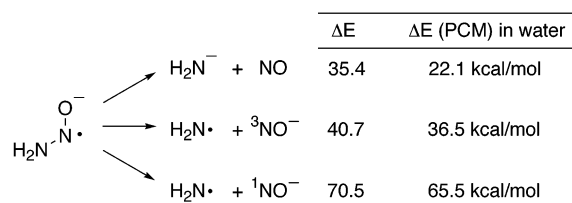
Proposed Mechanism of Photodecomposition. On the basis of product analysis, sensitization/quenching results, and the above calculations, we propose that the aqueous photodecom-

- (6) Murov, S. L.; Carmichael, I.; Hug, G. L. *Handbook of Photochemistry*, 2nd ed.; Marcel Dekker: New York, 1993; p 289.
- (7) (a) Foresman, J. B.; Head-Gordon, M.; Pople, J. A.; Frisch, M. J. *J. Phys. Chem.* **1992**, *96*, 135–149. (b) Bauernschmitt, R.; Ahlrichs, R. *Chem. Phys. Lett.* **1996**, *256*, 454–464. (c) Calculations were performed using the Gaussian 98 suite of programs: Frisch, M. J.; Trucks, G. W.; Schlegel, H. B.; Scuseria, G. E.; Robb, M. A.; Cheeseman, J. R.; Zakrzewski, V. G.; Montgomery, J. A., Jr.; Stratmann, R. E.; Burant, J. C.; Dapprich, S.; Millam, J. M.; Daniels, A. D.; Kudin, K. N.; Strain, M. C.; Farkas, O.; Tomasi, J.; Barone, V.; Cossi, M.; Cammi, R.; Mennucci, B.; Pomelli, C.; Adamo, C.; Clifford, S.; Ochterski, J.; Petersson, G. A.; Ayala, P. Y.; Cui, Q.; Morokuma, K.; Malick, D. K.; Rabuck, A. D.; Raghavachari, K.; Foresman, J. B.; Cioslowski, J.; Ortiz, J. V.; Stefanov, B. B.; Liu, G.; Liashenko, A.; Piskorz, P.; Komaromi, I.; Gomperts, R.; Martin, R. L.; Fox, D. J.; Keith, T.; Al-Laham, M. A.; Peng, C. Y.; Nanayakkara, A.; Gonzalez, C.; Challacombe, M.; Gill, P. M. W.; Johnson, B.; Chen, W.; Wong, M. W.; Andres, J. L.; Gonzalez, C.; Head-Gordon, M.; Replogle, E. S.; Pople, J. A. *Gaussian 98*, revision A.6; Gaussian, Inc.: Pittsburgh, PA, 1998.

Table 2. Geometrical Details for Diazeniumdiolate S_0 , S_1 , and T_1 States^a


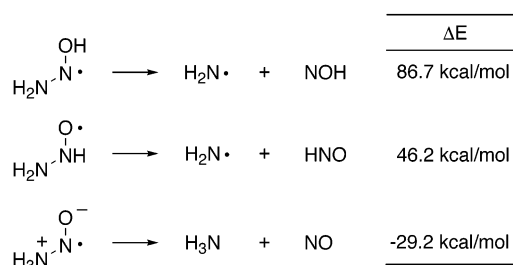
state	B1	B2	B3	B4	B5	B6	A1	A2
S_0	1.22	1.29	1.80	1.80	1.27	1.38	125.1	114.5
S_1 ($n-\pi^*$)	1.39	1.24	1.89	2.16	1.18	1.35	119.0	112.6
T_1 ($\pi-\pi^*$)	1.57	1.26	1.83	1.79	1.25	1.35	124.2	105.5

^aOptimized geometrical parameters (in Å and deg) of ground (HF/6-31+G(d,p)) and S_1 and T_1 excited states (CIS/6-31+G(d,p)) of Li^+ coordinated diazeniumdiolate.

**Figure 1.** Charges and spin densities (in parentheses) for diazeniumdiolate T_1 computed using natural population analysis at the B3LYP/6-31+G(d,p) level. (Structure is not completely optimized.)**Scheme 3****Scheme 4**

position of **3** proceeds via the reaction pathway shown in Scheme 3. Photoexcitation followed by intersystem crossing leads to ${}^3\mathbf{3}^*$, which subsequently dissociates to nitrosamine radical anion **5** and NO. Computational data on the parent nitrosamine radical anion (Scheme 4) suggest that **5** can potentially dissociate either to amide anion and NO or to aminyl radical and NO^- . B3LYP/6-31+G(d,p) calculations in the gas phase and with a PCM model⁸ for aqueous solvation suggest that dissociation to amide anion and NO is favored thermodynamically relative to formation of aminyl radical and NO^- . (Energies refer to the bottom-of-the-well values without the inclusion of zero-point vibrational energy correction.)

We further examined the protonation state of nitrosamine radical anion **5** in aqueous solution by computational methods. Using the method of Tomasi,⁹ we estimated the $\text{p}K_a$'s of the

Scheme 5

three possible protonated nitrosamine radical anions. Protonation on O and N of the nitroso unit leads to stable stationary points, and our calculations provide estimated $\text{p}K_a$ values of approximately 19. However, protonation on the amino N leads to spontaneous and barrierless fragmentation to ammonia and NO. To estimate a $\text{p}K_a$ value for the amino N-protonated nitrosamine radical anion, we fixed the N–N bond length at distances of 1.40, 1.47, and 1.52 Å and computed the $\text{p}K_a$'s of these partially constrained structures according to Tomasi's method. These calculations yielded $\text{p}K_a$ values of 11.8, 14.5, and 15.7, respectively. Because the N–N bond length of the nitrosamine radical anion is 1.52 Å, the most reasonable $\text{p}K_a$ estimate is 15.7. The thermodynamics of dissociation from each of these protonated species was also examined computationally (B3LYP/6-31+G(d,p) in the gas phase) and again indicates that dissociation to amine and NO is strongly favored (Scheme 5). The computed energetics based on the constrained geometry optimization of amino N-protonated nitrosamine radical anion, with the N–N distance fixed at 1.52 Å, suggests an exothermic dissociation. Interestingly, attempts to obtain a fully optimized geometry of the amino N-protonated nitrosamine radical anion resulted in a barrierless dissociation to generate ammonia and NO.

These results suggest that even at $\text{pH} = 12$ (typical of our experimental conditions) nitrosamine radical anion **5** is protonated and spontaneously dissociates to diethylamine and NO. Thus, the major photodecomposition pathway of **3** leads to diethylamine and 2 NO molecules, the same products observed upon thermal decomposition.¹

Because the formation of aminyl radical (which could subsequently be trapped by NO to give nitrosamine) and NO^-/HNO from **5** is predicted to be very unfavorable, we propose that nitrosamine and NO^- are formed via electron transfer from radical anion **5** to NO before cage escape (Scheme 3). This electron-transfer reaction from a triplet radical anion–radical pair to nitrosamine and ${}^3\text{NO}^-$ is predicted computationally (B3LYP/6-31+G(d,p)) to be exothermic by 10.2 kcal/mol in the gas phase. Experimentally, we estimate by cyclic voltammetry measurements that the reduction potential of *N*-nitroso-diethylamine is -2.0 ± 0.2 V versus normal hydrogen electrode. This estimate, together with the reported potential of -0.8 ± 0.2 V for the reduction of NO to ${}^3\text{NO}^-$,¹⁰ indicates that our proposed electron-transfer reaction is favored thermodynamically by approximately 25 kcal/mol.

Photolysis (Rayonet, 300 nm) of solutions saturated with NO had no effect on the yields of amine and nitrosamine (Table 1)

- (9) Schuurmann, G.; Cossi, M.; Barone, V.; Tomasi, J. *J. Phys. Chem. A* **1998**, *102*, 6706–6712.
 (10) Bartberger, M. D.; Liu, W.; Ford, E.; Miranda, K.; Switzer, C.; Fukuto, J. M.; Farmer, P. J.; Wink, D. A.; Houk, K. N. *Proc. Natl. Acad. Sci. U.S.A.* **2002**, *99*, 10958–10963.

(8) (a) Tomasi, J.; Persico, M. *Chem. Rev.* **1994**, *94*, 2027–2094. (b) Cramer, C. J.; Truhlar, D. G. *Chem. Rev.* **1999**, *99*, 2161–2200.

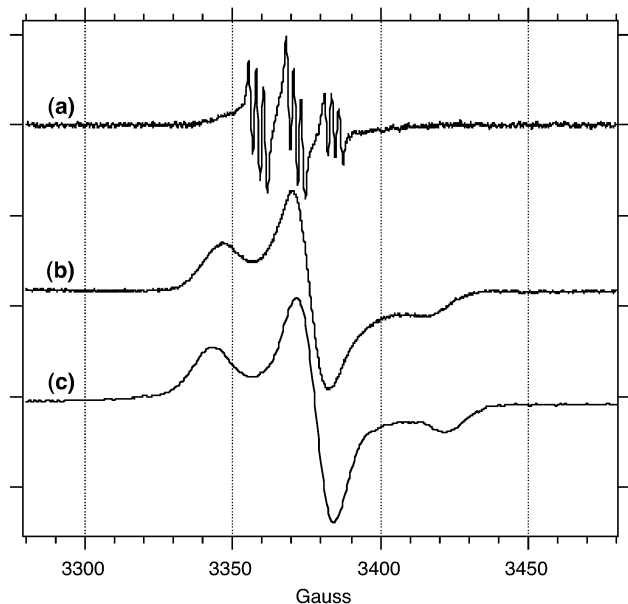


Figure 2. EPR spectra of (a) nitrosamine radical anion **5** (generated by potassium reduction of *N*-nitrosodiethylamine in THF) at room temperature, (b) nitrosamine radical anion **5** at 6 K, and (c) diazeniumdiolate **3** following brief photolysis at 6 K.

relative to those observed in argon-saturated solutions,¹¹ indicating that we are unable to trap radical anion **5** (by either chemical or electron-transfer reaction) once it escapes from the solvent cage, presumably due to its rapid dissociation to amine and NO. This observation is also consistent with the lack of reactivity of **5** with oxygen (Table 1). Indeed, we observe no evidence for bimolecular chemistry of nitrosamine radical anion **5** after cage escape.

There appears to be some wavelength dependence to the observed product distributions, with more nitrosamine (and presumably NO⁻) being formed following photolysis at 254 versus 300 nm. This may reflect a contribution by a competitive pathway from a higher lying singlet excited state leading directly to nitrosamine and ¹NO⁻. This potential contribution is currently under further investigation.

EPR Evidence for the Involvement of Nitrosamine Radical Anion 5. Nitrosamine radical anion **5** has been previously generated in room-temperature solutions of tetrahydrofuran (THF) by reduction of the corresponding nitrosamine on an alkali metal mirror and studied by EPR spectroscopy.¹² Following this work, potassium shavings were placed in a THF solution of *N*-nitrosodiethylamine and sealed in an EPR tube. The presence of nitrosamine radical anion **5** was suggested by the yellow-colored solution and confirmed by the room-temperature EPR spectrum shown in Figure 2a, which corresponds well to that reported previously.¹² The sample was then cooled to 6 K, and its EPR spectrum was again recorded (Figure 2b). A solution of diazeniumdiolate **3** in a perdeuterated methanol/ethanol (1:1) solution with added (0.1 M) perdeuterated methoxide was sealed in an EPR tube and cooled to 6 K.

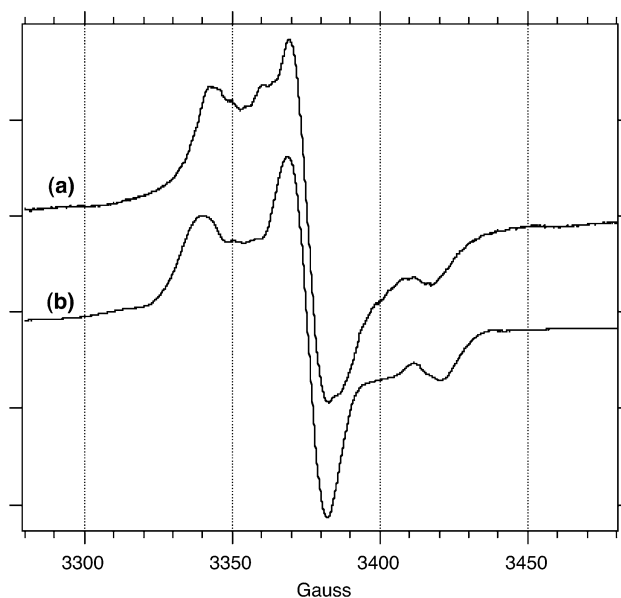


Figure 3. EPR spectra of (a) nitrosamine radical anion **5** following photolysis at 6 K and (b) diazeniumdiolate **3** following extended photolysis at 6 K.

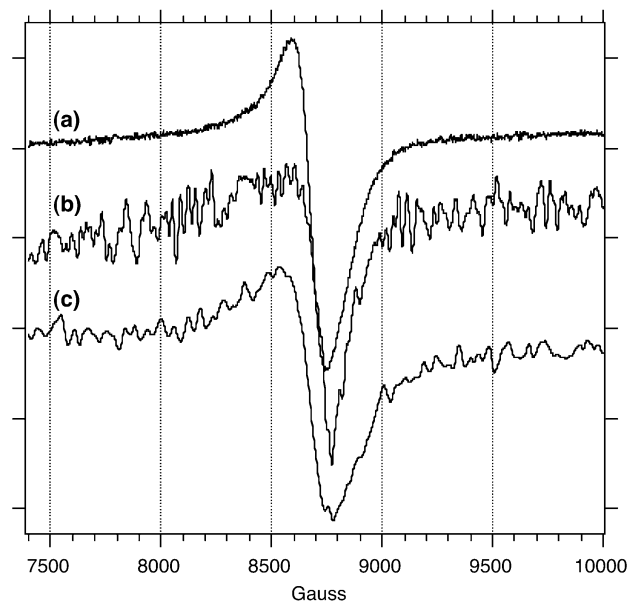


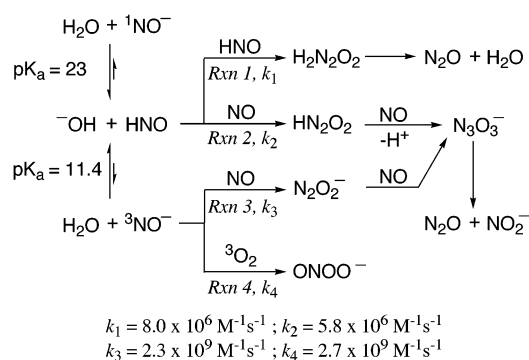
Figure 4. EPR spectra of (a) Angeli's salt **2** following photolysis at 6 K, (b) nitrosamine radical anion **5** following photolysis at 6 K, and (c) diazeniumdiolate **3** following extended photolysis at 6 K.

Brief photolysis yields the EPR spectrum shown in Figure 2c, which matches that of authentic nitrosamine radical anion **5**.

We further examined the photochemistry of nitrosamine radical anion **5** by low-temperature EPR spectroscopy (Figure 3a). This spectrum agrees well with that observed following extended photolysis of diazeniumdiolate **3** (Figure 3b). Moreover, in each case, an additional new signal is observed at high field (Figure 4). We believe that this signal may correspond to ³NO⁻ because photolysis of Angeli's salt **2** (see discussion below) in perdeuterated methanol/ethanol/water (1:1:1) frozen solution with added (0.1 M) perdeuterated methoxide provides the same signal (Figure 4a). Unfortunately, we are unaware of any reported EPR data on ³NO⁻ for comparison; however, the EPR spectrum of triplet oxygen (which is isoelectronic with

(11) NO was passed through a 5 M solution of aqueous NaOH and then through a drying tube filled with KOH and Drierite to remove trace contaminants of nitrogen dioxide. This purification is very important because experiments with unpurified NO lead to anomalously high yields of nitrosamine.

(12) (a) Stevenson, G. R.; Colon, C. J. *J. Phys. Chem.* **1971**, *75*, 2704–2705. (b) Stevenson, G. R.; Concepcion, J. G.; Castillo, J. J. *J. Phys. Chem.* **1973**, *77*, 611–614.

Scheme 6⁵

$^3\text{NO}^-$) has been studied in condensed phases.¹³ Signals for triplet oxygen have been observed by low-temperature EPR spectroscopy at 11 465 G (microwave frequency = 8.928 GHz) in a nitrogen matrix^{13a} and at 10 150 G (microwave frequency = 9.15874) in a deuterium matrix.^{13b} The signals of Figure 4 appear at 8665 G (microwave frequency = 9.48 GHz).

We, therefore, conclude that nitrosamine radical anion **5** is indeed formed upon photolysis of diazeniumdiolate **3** and that it can undergo photolysis itself to aminyl radical and $^3\text{NO}^-$. Because the relative yields of amine and nitrosamine in our room-temperature, solution-phase experiments do not depend on percent conversion or the intensity of the photolysis source (see Experimental Section for details), we do not believe that secondary photolysis of **5** is an important contributor to the results reported in Table 1.

Analysis of NO and NO⁻/HNO Yields. Our proposed mechanism (Scheme 3) necessitates a 1:1 ratio of nitrosamine: NO⁻/HNO and a 1:2 ratio of amine:NO. To quantify yields of NO⁻/HNO via N₂O or ONOO⁻ analysis, we relied on the model of the aqueous chemistry of NO⁻/HNO proposed by Shafirovich and Lymar in their recent studies of Angeli's salt photochemistry.⁵ As shown in Scheme 6,⁵ $^1\text{NO}^-$ is rapidly protonated ($\text{p}K_{\text{a}} = 20\text{--}23$) to form HNO. Slow spin-forbidden deprotonation of HNO to ground state $^3\text{NO}^-$ competes both with HNO dimerization (Reaction 1) and with HNO reaction with NO (Reaction 2). At $\text{pH} > 11.4$, formation of $^3\text{NO}^-$ becomes competitive; $^3\text{NO}^-$ can react with NO (Reaction 3) or with O₂ (Reaction 4).

According to Scheme 6, in argon-saturated solutions NO⁻/HNO can decompose to N₂O by three different pathways, two of which consume two molecules of NO (Reactions 2 and 3), and a third which consumes an additional molecule of HNO (Reaction 1). Thus, the amount of N₂O formed depends both on the pH (i.e., reaction of $^3\text{NO}^-$ or HNO) and on the relative reaction rates and concentrations of HNO and NO. At $\text{pH} = 12$, chemistry occurs predominantly from the more reactive $^3\text{NO}^-$ (Reaction 3) rather than from HNO (Reactions 1 and 2), and an approximately 1:1 ratio of nitrosamine:NO⁻/HNO (as N₂O) is observed (Table 1). Reaction 3 also consumes NO, resulting in NO yields (Table 1) that are less than those expected on the basis of Scheme 3 alone, but consistent with the above expectations.

In oxygen-saturated solutions at high pH, the formation of ONOO⁻ (Reaction 4) competes with Reactions 1, 2, and 3. Thus,

the yield of N₂O is diminished and ONOO⁻ is now observed under these conditions (Table 1). ONOO⁻ is not detected in argon-saturated solutions.

Conclusions

In summary, our results indicate that the photochemistry of 1-(*N,N*-dialkylamino)diazen-1-ium-1,2-diolates involves the formation of a nitrosamine radical anion and NO via a triplet excited state. The nitrosamine radical anion either undergoes electron transfer with NO before cage escape or dissociates to form ultimately amine and an additional molecule of NO. We are currently extending these investigations to determine if the photochemistry of other diazeniumdiolate derivatives X[N(O)-NO]⁻ (X = O⁻, CR₃, SO₃⁻) can be interpreted similarly.

Experimental Section

General Methods. Unless otherwise noted, materials were obtained from Aldrich Chemical Co. and used without further purification. Acetonitrile-*d*₃, deuterium oxide, and sodium deuterioxide (40 wt % solution in deuterium oxide) were used as received from Cambridge Isotope Laboratories. Acetonitrile was distilled from calcium hydride before use. ¹H NMR spectra were recorded on a Varian Unity Plus 400 (400 MHz) Fourier transform NMR spectrometer. Resonances are reported in δ units downfield from tetramethylsilane. Absorption spectra were obtained using a Hewlett-Packard 8453 diode array spectrophotometer. HPLC analysis was performed on a Waters Delta 600 System equipped with a model 6000A pump, a model 2487 dual wavelength UV detector, and a model U6K injector with a 20 μL injector loop (Rheodyne). A Waters C-18 Symmetry analytical column (3.9 \times 150 mm) was used. Nitrous oxide (N₂O) was analyzed using a Hewlett-Packard 5890 gas chromatograph equipped with an electron capture detector and an Alltech AT-molesieve capillary column (30 m \times 0.53 mm). Quantification of nitric oxide (NO) was performed electrochemically using an inNO Measuring System with an amiNO-700 probe (Innovative Instruments Inc.). The amiNO-700 probe was calibrated with sodium nitrite/ascorbic acid prior to use. Cyclic voltammetry experiments were performed using a CV-50W cyclic voltammetry system (Bioanalytical Systems Inc.) with a silver/silver nitrate reference electrode, a platinum mesh counter electrode, and a glassy carbon working electrode. EPR spectra were acquired on a Bruker EMX spectrometer operating at 9.48 GHz.

Sodium 1-(*N,N*-diethylamino)-diazen-1-ium-1,2-diolate (3**)** was prepared according to a literature procedure.¹⁴

Quantification of Diethylamine and *N*-Nitrosodiethylamine by ¹H NMR. Stock solutions of **3** were prepared to be 6.5 mM in D₂O/OD⁻ ($\text{pD} \geq 12$). Samples (1 mL) were sealed and purged for 5 min with Ar, O₂, or NO prior to photolysis (Rayonet, 254 or 300 nm), and then degassed with Ar after photolysis. NO was passed through a 5 M solution of aqueous NaOH and then through a drying tube filled with KOH and Drierite to remove trace contaminants of nitrogen dioxide. Photolysis times of approximately 5 min were necessary to reach ca. 30% conversion. The ratio of diethylamine to *N*-nitrosodiethylamine was determined by the relative integration of the methyl peaks ($\delta = 1.130$ ppm and 1.200, 1.472 ppm, respectively). Photolysis experiments (Rayonet, 350 nm) were performed analogously with triplet sensitizers. The sensitizers were added at a concentration of 1 mM (with approximately 1% acetonitrile-*d*₃ for solubility purposes) such that they absorbed >99% of the incident irradiation. The ratio of diethylamine to *N*-nitrosodiethylamine was not dependent on the percent decomposition of **3** nor on the intensity of the light source. Laser photolysis (Nd: YAG, 266 nm, 6 ns) of **3** with powers varying from 5 to 45 mJ/pulse

(13) For examples, see: (a) Kon, H. *J. Am. Chem. Soc.* **1973**, *95*, 1045–1049. (b) Kumada, T. *J. Chem. Phys.* **2002**, *117*, 10133–10138.

(14) Maragos, C. M.; Morley, D.; Wink, D. A.; Dunams, T. M.; Saavedra, J. E.; Hoffman, A.; Bove, A. A.; Isaac, L.; Hrabie, J. A.; Keefer, L. K. *J. Med. Chem.* **1991**, *34*, 3242–3247.

provided the same results (75% amine, 25% nitrosamine) within experimental error.

Quantification of *N*-Nitrosodiethylamine by HPLC. Stock solutions of **3** were prepared to be 100 μM in aqueous pH = 12 solution. Samples (3 mL) were purged with Ar or O₂ for 5 min in a sealed quartz cuvette prior to steady-state UV photolysis (Rayonet, 254 or 300 nm), and then degassed with Ar after photolysis. Photolysis times of approximately 10 s (254 nm) and 2 min (300 nm) were necessary to achieve ca. 30% conversion. Both photolyzed and unphotolyzed solutions were analyzed by HPLC; the mobile phase of methanol:water (60:40, v/v) with 0.1% added triethylamine at a flow rate of 0.6 mL/min allowed for virtually no decomposition of **3** on the column. The absolute amount of *N*-nitrosodiethylamine produced upon photolysis was determined from the percent decomposition of **3** and a calibration curve for *N*-nitrosodiethylamine.

Quantum Yield Determinations. Quantum yields for photodecomposition of **3** were determined at 266 nm (Nd:YAG) and 300 nm (Rayonet) using cycloheptadiene¹⁵ and azobenzene,¹⁶ respectively, as the actinometer. Sample solutions of **3** and the actinometer were made to have the same optical densities at the wavelength(s) of photolysis. Samples were sealed and purged for 5 min with Ar or O₂ prior to photolysis. Percent decomposition (typically less than 20%) was determined by HPLC for **3** and by a UV-vis spectroscopy for the actinometers.

Quantification of NO Released from the Photochemical Decomposition of **1.** Stock solutions of **1** were prepared to be 1 μM in aqueous pH = 12 solution. Samples (3 mL) were added to a sealed quartz cuvette equipped with a stirbar such that there was no headspace. The amiNO-700 probe was inserted through the top of the cap. The probe was allowed to equilibrate in the sample solution prior to steady-state photolysis (Xe-Arc lamp, unfiltered or >285 nm). Given the broad output of the Rayonet bulbs (254 nm, ca. 240–270 nm; 300 nm, ca. 270–350 nm) and the relative extinction coefficients of **3** in the UV region (Figure S2), these photolysis conditions reasonably approximate Rayonet photolysis at 254 or 300 nm, respectively. No signal was observed prior to photolysis, but a steadily increasing signal was observed upon irradiation. The focal point of the light was kept 2 cm above the tip of the probe to avoid artifacts due to the photoelectric effect. Photolysis times of 2–4 min were required to achieve 5–30% conversions. To determine percent conversion, the sample cell was opened to the air and the photogenerated NO was allowed to diffuse out of solution. The probe was allowed to equilibrate once more before the remaining **3** was thermally decomposed by the addition of 10 μL of 1 M H₂SO₄. As a calibration, 1 μM stock solutions of **3** were thermally decomposed several times, and an average value for total NO release was obtained. The absolute amount of NO generated was then determined on the basis of the amount of NO released photochemically, the fact that **3** decomposes thermally to 1.5 eq of NO,¹⁴ and the calibration data.

Quantification of N₂O Generated from the Photochemical Decomposition of **3.** Stock solutions of **1** were prepared to be 1 mM in aqueous solution at pH = 12. Samples (3 mL) were purged with Ar for 10 min in a sealed quartz cuvette prior to steady-state UV photolysis (Rayonet, 254 nm). Photolysis times of 15 min were necessary to achieve 100% conversion. N₂O was sparged to a cold trap immersed in liquid nitrogen, and then volatilized into a gas chromatograph (AT-molesieve capillary column, 30 m \times 0.53 mm, Alltech Associates) where it was then separated from other volatile species. N₂O was quantified with an electron capture detector, which was calibrated with an authentic standard prior to the experiment.

Quantification of Peroxynitrite Generated from the Photochemical Decomposition of **3.** Stock solutions of **1** were prepared to be 200 μM in aqueous solution at pH = 14. Steady-state UV photolysis

(Rayonet, 254 nm) of 3 mL aliquots in oxygen saturated solutions resulted in the rapid disappearance of the absorption band at 248 nm and concomitant appearance of characteristic absorption of ONOO⁻ at 302 nm ($\epsilon = 1670 \text{ M}^{-1} \text{ cm}^{-1}$).¹⁷ A well-defined isosbestic point was observed at 283 nm. The yield of peroxynitrite was calculated on the basis of 100% conversion of **3** and the molar absorptivity of peroxynitrite.

EPR Studies of the Photoreactivity of **3.** Sample solutions of **3** were prepared to be 10–20 mM in 1:1 perdeuterated methanol:ethanol with 0.1 M added perdeuterated methoxide and were subjected to three freeze–pump–thaw cycles before being sealed under vacuum in 4 mm quartz tubes. Samples were cooled by a continuous flow of helium using an Oxford ESR-900 cryostat with a model ITC 503 temperature controller. Samples were irradiated at 6 K for 1–2 min using focused UV light from a 250 W Oriel Hg-arc lamp. Spectra were recorded both before and after UV irradiation to allow for subtraction of background.

Independent Generation of *N*-Nitrosodiethylamine Radical Anion (5**).** The radical anion of **5** was generated according to the method of Stevenson and co-workers.¹² Freshly cut potassium shavings were added to a 4 mm quartz tube containing a 15 mM solution of *N*-nitrosodiethylamine in freshly distilled THF. Samples were subjected to three freeze–pump–thaw cycles before being sealed under vacuum. The room-temperature spectrum was reproduced for verification before recording the spectrum at 6 K.

Estimation of the Reduction Potential of *N*-Nitrosodiethylamine. Solutions of *N*-nitrosodiethylamine were made to be 0.01 M in dry DMF with added 0.01 M ferrocene (as an internal standard¹⁸) and added 0.1 M tetrabutylammonium perchlorate (as supporting electrolyte). Solutions were purged with He for 2 min prior to each run. Current versus potential data curves were collected at scan rates of 100, 200, 300, 400, and 500 mV/s beginning at 800 mV with a switching potential of –2800 mV. (See Supporting Information.) Reduction of the nitrosamine was observed to be completely irreversible; thus, only an estimate of the true reduction potential is possible.¹⁹ The onset of current increase as a function of scan rate was used to estimate the reduction potential of *N*-nitrosodiethylamine (–2.0 \pm 0.2 V vs normal hydrogen electrode, calibrated with the internal ferrocene reduction potential in DMF¹⁸). The relative peak amplitudes corresponding to ferrocene and *N*-nitrosodiethylamine confirmed the reduction of the latter to be a one-electron process.

Computational Methods. Geometries were fully optimized for the singlet ground state for both lithium ion coordinated and anionic diazeniumdiolates at the Hartree–Fock and the hybrid B3LYP density functional theory with the 6-31+G(d,p) basis set.²⁰ These stationary points in the gas phase were characterized by vibrational frequency analyses as minima on their respective potential energy surfaces. Calculations on triplet states were performed using the unrestricted molecular orbital formalism. Vertical excitation energies were evaluated on optimized geometries by the configuration interaction with all single excitations method (CIS) and by time-dependent density functional theory method (TD-DFT)²¹ with the B3LYP functional. After all of the vertical excitations were carefully analyzed, geometries for states of interest were optimized at the CIS/6-31+G(d,p) level. Atomic charges

(15) Numao, N.; Hamada, T.; Yonemitsu, O. *Tetrahedron Lett.* **1977**, *19*, 1661–1664.

(16) Gauglitz, G.; Hubig, S. *J. Photochem.* **1985**, *30*, 121–125.

(17) (a) Hughes, M. N.; Nicklin, H. G. *J. Chem. Soc. A* **1968**, 450–452. (b) Schmidt, K.; Kalt, P.; Mayer, B. *Biochem. J.* **1994**, *301*, 645–647.

(18) Noviadri, I.; Brown, K. N.; Fleming, D. S.; Gulyas, P. T.; Lay, P. A.; Masters, A. F.; Phillips, L. *J. Phys. Chem. B* **1999**, *103*, 6713–6722.

(19) Bard, A. J.; Faulkner, L. R. *Electrochemical Methods Fundamentals and Applications*; John Wiley & Sons: New York, 2001.

(20) (a) Hehre, W. J.; Radom, L.; Schleyer, P. v. R.; Pople, J. A. *Ab Initio Molecular Orbital Theory*; Wiley: New York, 1986. (b) Becke, A. D. *J. Chem. Phys.* **1992**, *97*, 9173–9177. (c) Becke, A. D. *J. Chem. Phys.* **1993**, *98*, 5648–5652. (d) Lee, C.; Yang, W.; Parr, R. G. *Phys. Rev.* **1988**, *B37*, 785–789. (e) Becke, A. D. *Phys. Rev.* **1988**, *A38*, 3098–3100. (f) Stephens, P. J.; Devlin, F. J.; Chablowski, C. F.; Frisch, M. J. *J. Phys. Chem.* **1994**, *98*, 11623–11627.

(21) (a) Gross, E. K. U.; Kohn, W. *Adv. Quantum Chem.* **1990**, *21*, 255–91. (b) Bauernschmitt, R.; Ahlrichs, R. *Chem. Phys. Lett.* **1996**, *256*, 454–464. (c) Bauernschmitt, R.; Haeser, M.; Treutler, O.; Ahlrichs, R. *Chem. Phys. Lett.* **1997**, *264*, 573–578.

were evaluated using the natural population analysis method.²² The effect of solvation has been taken into account with the self-consistent reaction field method and the polarizable continuum models of Tomasi and co-workers.⁸ All calculations were performed using the Gaussian 98 suite of programs^{7c} at the Ohio Supercomputer Center.

Acknowledgment. We gratefully acknowledge the National Institutes of Health (at Hopkins) and National Science Foundation and the Ohio Supercomputer Center (at Ohio State) for generous support of this research. J.P.T. also acknowledges a Camille Dreyfus Teacher-Scholar Award and an Alfred P. Sloan Research Fellowship. C.M.P. acknowledges a Peter F. Bronfman International Scholarship. We thank Lev R. Ryzhkov for helpful

discussions and also thank Larry K. Keefer, Steven Fox, and Brett M. Showalter for assistance with N₂O quantification and Gerald J. Meyer for assistance with electrochemical measurements.

Supporting Information Available: Optimized geometries, energies, orbital contour plots, computed vertical excitation energies (eV and nm), and oscillator strengths, the experimental absorption spectrum of **3**, and electrochemical data used to estimate the reduction potential of *N*-nitrosodiethylamine (PDF). This material is available free of charge via the Internet at <http://pubs.acs.org>.

(22) Reed, A. E.; Curtiss, L. A.; Weinhold, F. *Chem. Rev.* **1988**, 88, 899–926.

JA034487Y